JOC The Journal of Organic Chemistry

Article

pubs.acs.org/joc

Theoretical Investigations on the Mechanism of Dual 1,3-Dipolar Cycloaddition of CO_2 with Isocyanides and Alkynes

Weiyi Li,*[,†] Dongfeng Huang,[‡] and Yajing Lv[†]

[†]School of Physics and Chemistry, Research Center for Advanced Computation, Xihua University, Chengdu, Sichuan 610039, People's Republic of China

[‡]College of Chemistry and Chemical Engineering, Anyang Normal University, Anyang, Henan 455000, People's Republic of China

Supporting Information

ABSTRACT: The mechanism of dual 1,3-dipolar cycloaddition reaction of CO_2 with isocyanides and alkynes was studied using DFT calculations. The calculations show that this three-component reaction takes place from the nucleophilic attack of isocyanides to alkynes with the generation of 1,3-dipolar active species, which requires the largest energy barrier (24.3 kcal mol^{-1}) and can be regarded as the rate-determining step for the entire reaction. From 1,3-dipolar species, the desired spiro compound is obtained through the energy-favorable dual 1,3-dipolar cycloaddition channel, including successive asynchronous concerted cycloaddition of CO_2 with the 1,3-dipole and cycloaddition of 1,3-dipole with the resultant lactone. Additionally, the competing nucleophilic addition of 1,3-dipole with alkynes could lead to the production of 1,5-dipolar intermediate, which will alternatively react with isocyanides or CO_2 and generate several byproducts. The investigations on the substituent effect of both substrates indicate that the substituents on alkynes play the more significant roles in controlling the rate and selectivity of the reaction than those on isocyanides. The moderate electron-withdrawing and conjugate groups on alkynes not only favor the generation of the 1,3-dipole, but also stabilize the negative charge on these species without losing reactivity.

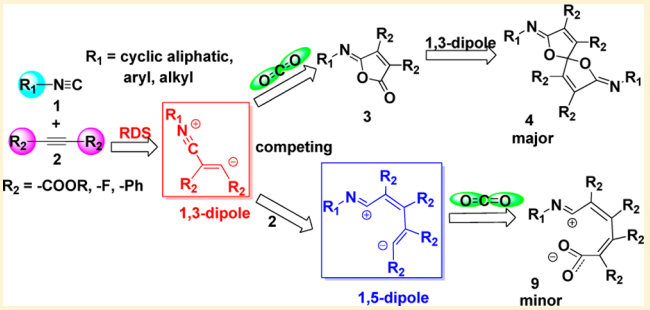

1. INTRODUCTION

Currently, chemical fixation of CO_2 is attracting a great deal of interest,[1] because it is one of the potential protocols to reduce the concentration of CO_2 in the atmosphere. On the other hand, CO_2 is also regarded as a highly abundant, inexpensive, nontoxic, nonflammable, and renewable carbon resource. The development of environmentally friendly and economical methodologies for the incorporation of CO_2 as C_1 feedstock into value-added chemicals is highly desirable from the viewpoint of green and sustainable chemistry.[2]

Although great progress of the transformation of CO_2 into chemical products was achieved in the past few decades, the scope of the synthetic applications of CO_2 is limited due to its high thermodynamic stability and kinetic inertness. In general, chemical fixation of CO_2 can be classified into three categories (Scheme 1): (i) as an electrophile, CO_2 can be activated by the strong nucleophiles, such as Grignard reagents, small-membered ring compounds,[3] and *N*-heterocyclic carbene,[4] leading to the production of carboxylic acids or carboxylates; (ii) as an "anhydrous carbonic acid", CO_2 can react with basic compounds like NH_3, amines, and other amino compounds,[5] resulting in ureas,[6] oxazolidinones,[7] quinazolines,[8] carbamates,[9] and isocyanates[10] through the construction of C−N bonds; and (iii) because CO_2 is at the highest oxidation state carbon,[11] it can be reduced by H_2, silanes, hydroboranes, and metal−hydrides to fuel molecules, such as CO,[12] CH_3OH,[13] and CH_4.[14] To the best of our knowledge, apart from the reduction reaction, one C═O bond of CO_2 is transformed to other functional groups, while the other one remains as a carbonyl group in the almost reported cases. The examples of both C═O bonds of CO_2 reacting in one reaction are rather rare.

Scheme 1. General Strategies for CO_2 Transformation

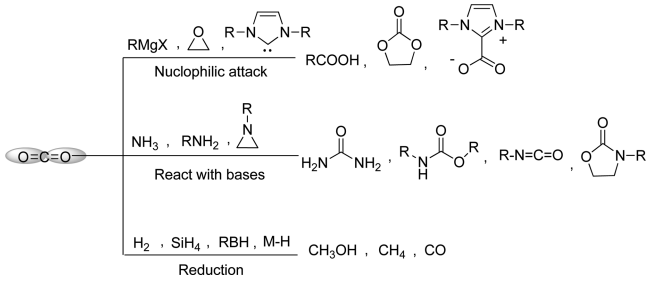

Very recently, Wang, Ji, and their co-workers[15] reported the first case of two C═O bonds of CO_2 simultaneously reacting in one reaction, affording symmetric spiro compound from dual 1,3-dipolar cycloaddition reaction of CO_2 with isocyanide **1a**

Received: July 28, 2014
Published: October 23, 2014

   dx.doi.org/10.1021/jo5017053 | J. Org. Chem. 2014, 79, 10811−10819

Scheme 2. Cycloaddition of CO_2 with Isocyanides and Dimethyl Acetylenedicarboxylates

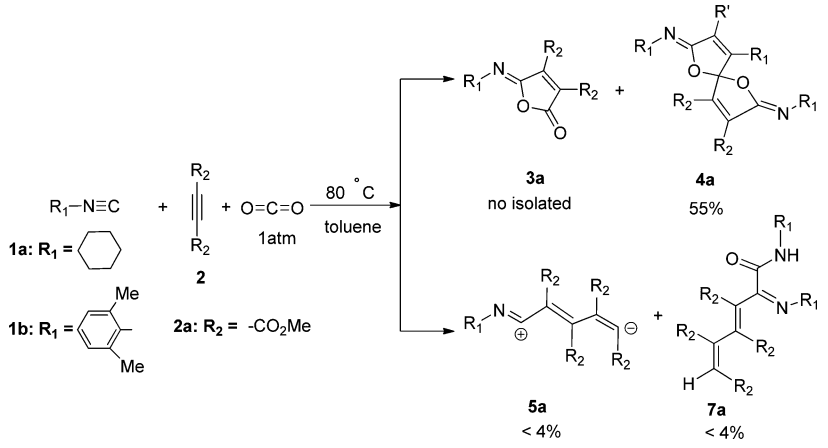

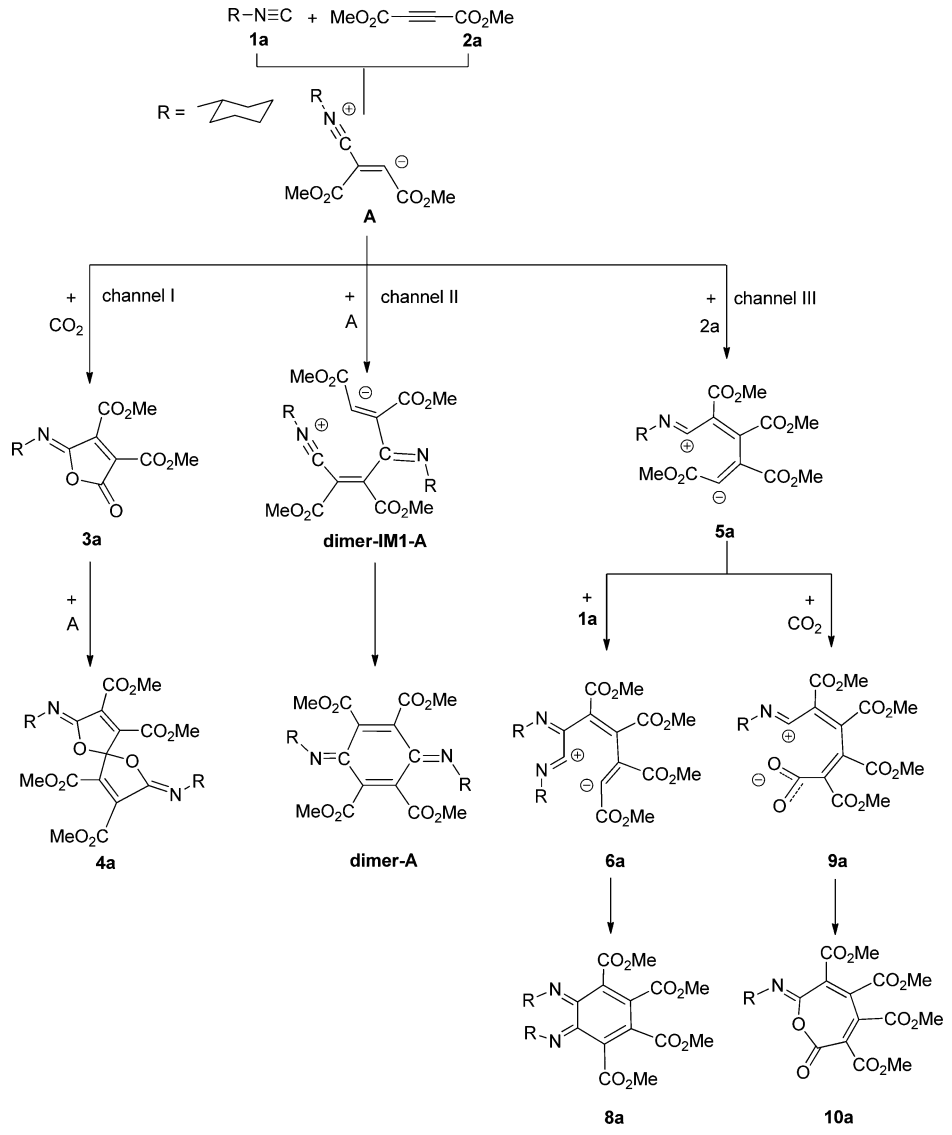

Figure 1. Reaction channels for the major product and side-products in cycloaddition of CO_2 with **1a** and **2a**.

and dimethyl acetylenedicarboxylates **2a** (Scheme 2). Under the optimal reaction conditions (80 °C, pressure of 1 atm for CO_2, toluene solvent), dual cycloaddition product 1,6-dioxospiro[4,4]nonane-3,8-diene **4a** was obtained with moderate isolated yield (55%). The side-products 1,5-dipolar intermediate **5a** as well as the hydrolysis product **7a** were observed with the yield of less than 4%. In addition, a number of isocyanides and the conjugated triple bond acceptors bearing

dx.doi.org/10.1021/jo5017053 | J. Org. Chem. 2014, 79, 10811−10819

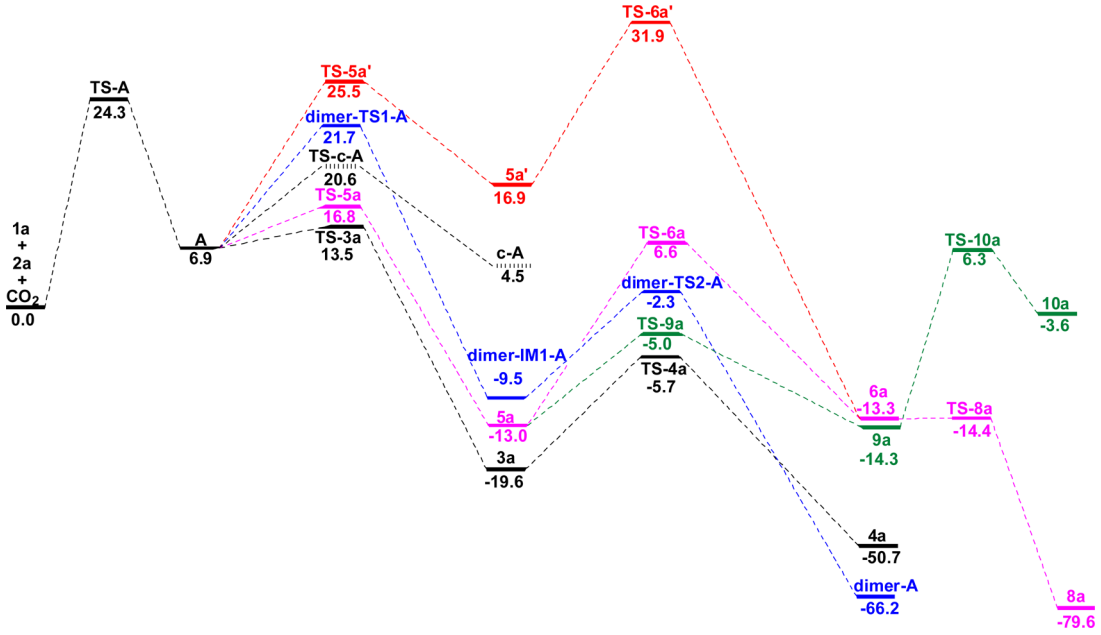

Figure 2. Energy profiles of cycloaddition of CO_2 with **1a** and **2a**. The relative free energies (in kcal mol^{-1}) involve Gibbs free energy corrections at 298 K in the gas phase, single-point energies in toluene, and DFT-D3 dispersion corrections.

the various kinds of substituent groups were also investigated. Among these, the best result (yield of 60%) for dual cycloaddition product was achieved when 1,3-dimethylbenzyl isocyanide (**1b**) and diethyl acetylenedicarboxylate were used in the reaction.

On the basis of the experimental results, two plausible reaction channels were proposed for the major product **4a** and the side-product **7a**, respectively.[15] However, due to the difficulty in isolating and identifying the key intermediates, such as the 1,3-dipolar intermediate, mono 1,3-dipolar cycloaddition intermediate, and 1,5-dipolar intermediate, the overall reaction mechanism is still uncertain. Herein, we carried out a comprehensive theoretical investigation on the title reaction (Scheme 2) to further understand the mechanism of this novel reaction at a molecular level. In the present work, the detailed reaction channels leading to the different products as well as the substituent effect of isocyanides and alkynes on the reaction were explored by the combination of DFT calculations and electronic effect analysis, aiming to get insight into the factors that controlled the reaction rate, the selectivity to the final products, and the substrate scope in the present synthetic methodology for the chemical fixation of CO_2.

2. COMPUTATIONAL METHODS

For the investigated reaction system, the geometric optimizations of all reactants, intermediates, transition states, and products were performed using Becke's three parameter exchange function and the nonlocal correlation functional of Lee, Yang, and Parr (B3LYP[16]) with the 6-31+G* basis set.[17] The harmonic frequencies were calculated at the same level to obtain the Gibbs free energy corrections (G_c) in the gas phase at 298.15 K and 1 atm. The optimized structures were characterized as minima (no imaginary frequency) or transition states (with one unique imaginary frequency) by vibrational mode analysis. The energies were then improved by the B3LYP/6-311++G** single-point calculations in toluene solvent (experimentally used) with the SMD[18] continuum solvation model. To consider the dispersion effect, Grimme's DFT-D3 (BJ-damping function) dispersion corrections were calculated by employing the DFTD3 program.[19] To assess the computed results obtained from the above methods, some representative transition states were recalculated at the M06-2X(SMD, toluene)/6-311++G**//M06-2X/6-31+G* level. The comparisons showed that B3LYP and M06-2X produced similar optimized geometries. The final conclusions are also the same with both methods (see section S3 in the Supporting Information). Furthermore, Natural Bond Orbital (NBO[20]) analysis on the optimized structures was carried out to get a further insight into the electronic properties of the system. The reactivity indices (global electrophilicity index ω and nucleophilicity index N)[21,22] of the reactants and intermediates involved in the cycloaddition reaction were also performed by computing the HOMO and LUMO energies of the ground states of the molecules. Because commonly used DFT functionals may not predict orbital energies accurately, TD-DFT method was employed to obtain the accurate LUMO eigenvalues and HOMO−LUMO gaps.[23] All calculations were performed using the Gaussian 09 program.[24] The figures of three-dimensional molecular structures were drawn using the CYLVIEW program.[25]

3. RESULTS AND DISCUSSION

3.1. Overall Reaction Mechanism. In this section, the overall mechanism for the reaction of CO_2 with the isocyanide **1a** and dimethyl acetylenedicarboxylate **2a** was explored to prove the important intermediates proposed in the experiment and gain the energetic properties for the generation of the major and side-products. According to the experimental observation[15] and the related literature,[26] we predict that this three-component reaction system initially takes place from the nucleophilic addition of **1a** with **2a** with the formation of the highly reactive zwitterionic intermediate **A**, which behaves as the 1,3-dipolar species (Figure 1). From the highly active 1,3-dipole **A**, there are three parallel reaction channels leading to the different products: (i) production of the spiro compound **4a** via two successive 1,3-dipolar cycloaddition reactions (channel I), (ii) dimerization of 1,3-dipolar **A** via the homocoupling process (channel II), and (iii) generation of 1,5-dipolar intermediate **5a** followed by the electrophilic addition with **1a** or nucleophilic attack of CO_2, resulting in intermediate **6a** or carboxylation product **9a** (channel III). The

dx.doi.org/10.1021/jo5017053 | J. Org. Chem. 2014, 79, 10811−10819

computed potential energy surfaces (PESs) of these three reaction channels are illustrated in Figure 2.

Formation of 1,3-Dipole ***A***. Because chemical reactivity indices defined with the framework of DFT are powerful tools in understanding the electronic properties of the system, electronic chemical potential μ, chemical hardness η, global electrophilicity ω, and global nucleophilicity N of the reactants were calculated using TD-DFT method and presented in the Supporting Information. From Supporting Information Table S2, the electronic chemical potential of the isocyanide **1a** (μ = −4.89 eV) is higher than that of **2a** (μ = −6.14 eV), suggesting that the net charge transfer (CT) in the formation of 1,3-dipole **A** will take place from isocyanide **1a** toward **2a**. From the visualized molecular orbitals of the reactants **1a** and **2a** (in Figure 3), it can be seen that the electron is transferred from

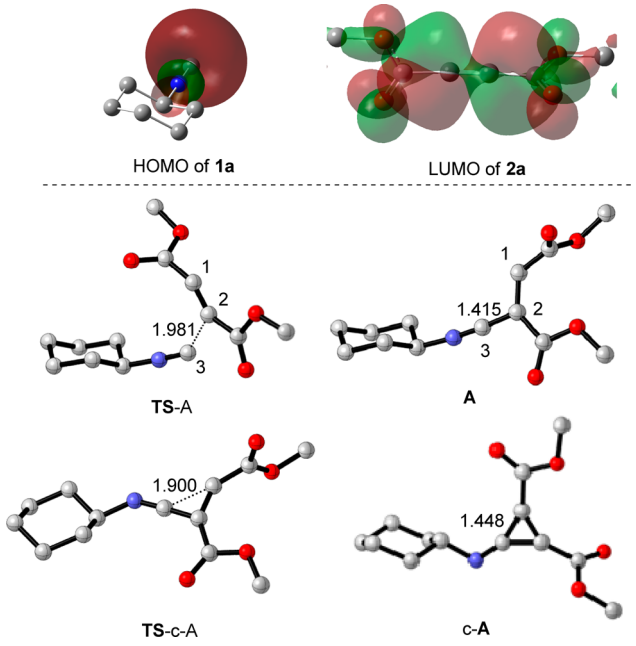

Figure 3. Visualization of molecular orbitals of the reactants, and the optimized structures of the species involved in the formation of 1,3-dipole **A**.

the lone pair of the C3 atom in the HOMO of **1a** to the empty π orbital of the C3 atom in the LUMO of **2a**. When the C3 atom of **1a** approaches the C2 atom of **2a**, the forming C−C bond distance in transition state **TS**-A is 1.981 Å, and the net CT from **1a** moiety to **2a** moiety is 0.05 *e*. The energy barrier for the generation of 1,3-dipole **A** is calculated to be 24.3 kcal mol^{-1} at the B3LYP(SMD, toluene)/6-311++G**//B3LYP/6-31+G* level with the inclusion of DFT-D3 dispersion energy correction. The higher energy barrier (28.8 kcal mol^{-1}) of this process is predicted by the M06-2X method. The whole process is endergonic by 6.9 kcal mol^{-1}, and the isomerization of 1,3-dipole **A** to the inactive species c-**A** via the three-membered-ring transition state **TS**-c-A requires an energy barrier of 13.7 kcal mol^{-1}.

Channel I: Formation of Dual 1,3-Dipolar Cycloaddition Product. From Figure 4, it is shown that the largest contribution to the HOMO of 1,3-dipole **A** is from the lone pair of the C1 atom, which could give high overlapping with the LUMO of CO_2 molecule in the fashion of 1,3-dipolar cycloaddition. The energy gap between the LUMO of CO_2 and the HOMO of 1,3-dipole **A** is calculated to be 5.1 eV,

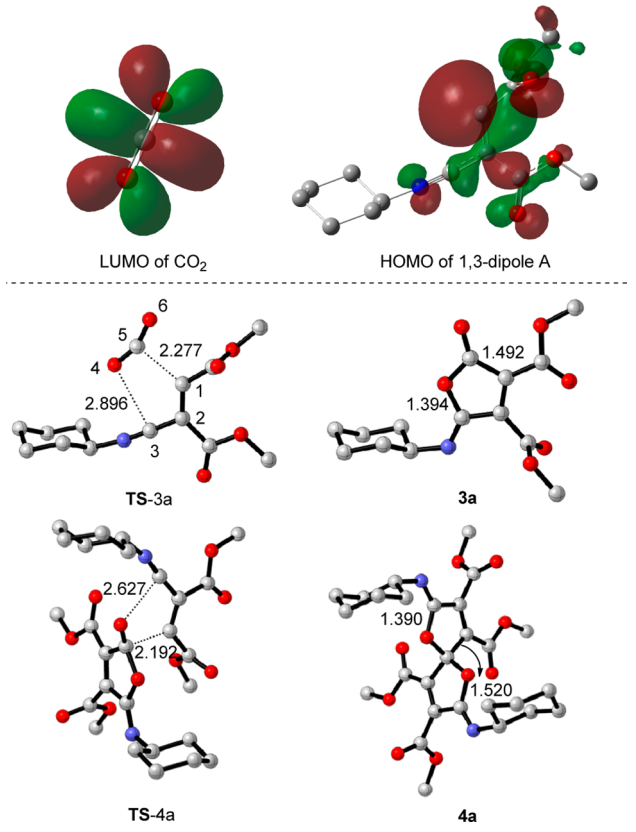

Figure 4. Visualization of molecular orbitals of the reactants, and the optimized structures of species involved in dual cycloaddition reaction channel.

indicating that the nucleophilic addition of 1,3-dipole **A** to CO_2 is feasible. The nucleophilic attack of 1,3-dipole **A** with CO_2 then takes place via the cycloaddition transition state **TS**-3a. In transition state **TS**-3a, the distances of the forming C1−C5 and C3−O4 bonds are 2.277 and 2.869 Å, respectively, while the net CT from 1,3-dipole **A** moiety to CO_2 moiety is 0.20 *e*. These results point out that the cycloaddition transition state **TS**-3a is asynchronous with high polarity. The energy barrier of this cycloaddition step is calculated to be 7.1 kcal mol^{-1} lower than the one along the isomerization pathway, meaning that the cycloaddition of 1,3-dipole **A** with CO_2 is much more favorable than the isomerization of 1,3-dipole A to inactive species. Downhill from transition state **TS**-3a, the five-membered-ring lactone **3a** is constructed with the fixation of CO_2. Because of the presence of the conjugate π electrons in **3a**, the biradicaloid resonance structures corresponding to the localization of radicals on the oxygen atom, nitrogen atom, or carbon atom are possible. The computational investigations on the structure of **3a** using DFT (B3LYP, M06-2X, BP86, B97D, and BPW91 functionals) and MP2 ab initio methods indicate that the lactone **3a** is more stable in closed-shell ground state, which rules out the possibility that **3a** might exist in the form of the biradicaloid structure (see section S4 in the Supporting Information). On the basis of the chemical reactivity index analysis, intermediate **3a** can be classified as a strong electrophile (ω = 5.87 eV). The remaining carbonyl group of **3a** then can continue to react with the nucleophile 1,3-dipole **A** via transition state **TS**-4a, affording the dual cycloaddition product **4a**. In transition state **TS**-4a, the distance of forming C1−C5 and C3−O4 bonds is 2.627 and 2.192 Å, respectively.

dx.doi.org/10.1021/jo5017053 | J. Org. Chem. 2014, 79, 10811−10819

The CT from 1,3-dipole **A** fragment to **3a** moiety is 0.37 *e*. These results suggest that transition state **TS**-4a also exhibits the pronounced character of asynchronicity and polarity. The energy barrier of this cycloaddition step is calculated as 13.9 kcal mol^{-1}, indicating this cycloaddition process is kinetically feasible under ambient temperature. Finally, the spiro compound **4a** is yielded, lying 50.7 kcal mol^{-1} below that of reactants. Because the dual cycloaddition product **4a** is 31.1 kcal mol^{-1} more stable than mono cycloaddition product **3a** in thermodynamics, the transformation from **3a** to **4a** can spontaneously take place through this cycloaddition process. The calculation reasonably accounts for the experimental observation that the isolation of the mono cycloaddition intermediate **3a** was difficult under the present condition.[15]

Channel II: Homocoupling of Two 1,3-Dipole A. Alternatively, because 1,3-dipole **A** has high reactivity, the formation of the dimeric species via the homocoupling of 1,3-dipole **A** monomer was considered. The calculations suggest that the dimerization of 1,3-dipole **A** monomer proceeds through a two-step mechanism rather than the one-step concerted mechanism one may expect. In the first step, the electropositive C3 atom approaches the electronegative C1 atom via the intermolecular electrophilic addition transition state dimer-**TS1**-**A**, resulting in another zwitterionic intermediate dimer-**IM1**-**A** (Figure 5). In dimer-**TS1**-**A**, the distance

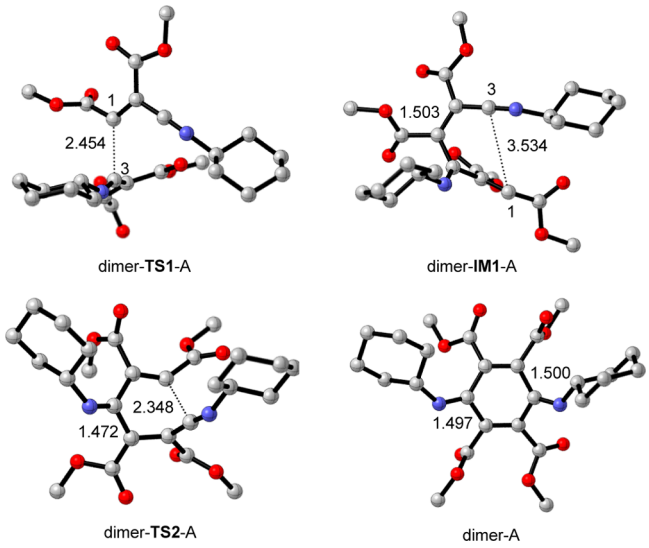

Figure 5. Optimized structures of the species involved in the homocoupling reaction channel.

of the forming C1−C3 bond is 2.454 Å, and the net CT between these two fragments is 0.20 *e*. Dimer-**TS1**-**A** is only 2.3 kcal mol^{-1} higher than the separated 1,3-dipole A monomer in enthalpy, but the free energy of dimer-**TS1**-**A** is increased to 14.8 kcal mol^{-1} due to the entropic penalty. After the pathway crosses transition state dimer-**TS1**-**A**, the C1−C3 bond is formed in intermediate dimer-**IM1**-**A** with a shorter bond length of 1.503 Å. The zwitterionic character of dimer-**IM1**-**A** is weaker than that of 1,3-dipole **A** monomer, as suggested by the lower positive charge on the C3 atom (0.60 *e* vs 0.65 *e*). Hence, intermediate dimer-**IM1**-**A** is 15.4 kcal mol^{-1} more stable than 1,3-dipole **A** monomer in thermodynamics. Subsequently, dimer-**IM1**-**A** could undergo an intramolecular electrophilic attack to give the dimeric species dimer-**A** by crossing a low energy barrier (dimer-**TS2**-**A**) of 7.2 kcal mol^{-1}. In transition state dimer-**TS2**-**A**, the distance of the C1−C3 bond shortens from 3.534 (in dimer-**IM1**-**A**) to 2.348 Å. The formation of the dimeric cycloaddition product dimer-**A** is overall exergonic by 66.2 kcal mol^{-1}, suggesting this dimerization process is thermodynamically preferable. As compared to the cycloaddition of 1,3-dipole **A** with CO_2, the relative free energy of transition state dimer-**TS1**-**A** is 8.2 kcal mol^{-1} higher than that of **TS**-3a, indicating the dimerization of 1,3-dipole **A** is kinetically inferior to the cycloaddition of 1,3-dipole **A** with CO_2.

Channel III: Formation of 1,5-Dipolar Intermediate. In addition to the above two reaction channels, 1,3-dipole **A** also called attention to the possible channel for producing 1,5-dipolar intermediate **5a** due to the possibility that the reaction of 1,3-dipole A with **2a** could compete with the 1,3-dipolar cycloaddition of this species with CO_2. Along this reaction channel, two different paths have been considered to account for the generation of zwitterionic intermediate **6a**. The difference between these two paths lies in the reaction sequence of 1,3-dipole **A** with **1a** and **2a** (see Figure S3 in the Supporting Information). The energetic comparison between these two paths shows that the prior reaction of **2a** with 1,3-dipole **A** followed by the reaction of **1a** is energetically more preferable (Figure 2). This might be attributed to two facts: (i) the electrophilicity of **2a** is higher than that of **1a**, and (ii) the HOMO of 1,3-dipole **A** could give higher overlap with the LUMO of **2a** (Figure 6). For a concise expression, the energy-favorable path is discussed in the following.

As shown in Figure 6, when the external **2a** gets close to 1,3-dipole **A**, the nucleophilic attack of the electronegative C1 to the C7 atom of **2a** occurs via transition state **TS**-5a, allowing the formation of 1,5-dipolar intermediate **5a**. In transition state **TS**-5a, the forming C1−C7 bond distance is 2.218 Å, and the CT from 1,3-dipole **A** moiety to **2a** moiety is 0.28 *e*. Relative to the separated reactants, the enthalpy of **TS**-5a is 3.0 kcal mol^{-1}, but the free energy of **TS**-5a raises up to 16.8 kcal mol^{-1} due to entropy loss. The energy barrier of this step is 3.3 kcal mol^{-1} (4.6 kcal mol^{-1} at the M06-2X/(SMD, toluene)/6-311++G**//M06-2X/6-31+G* level) more unfavorable than the 1,3-dipolar cycloaddition of CO_2 over **TS**-3a. Thus, the computational result obtained from B3LYP/B3LYP-D3 method could more reasonably account for the experimental observation that a small quantity of 1,5-dipolar intermediate **5a** was yielded.[15] Similar to 1,3-dipole **A**, the resultant 1,5-dipole **5a** also exhibits a zwitterionic character, as evidenced by the large dipole moment (5.212 D) and negative charge accumulated on the newly formed **2a** fragment (−0.46 *e*). Meanwhile, 1,5-dipole **5a** presents both strong electrophilicity (ω = 3.75 eV) and nucleophilicity (N = 4.64 eV), which might alternatively react with isocyanide **1a** or CO_2 in the subsequent process.

When the isocyanide **1a** approaches 1,5-dipole **5a**, the electrophilic addition takes place via transition state **TS**-6a, in which the forming C3−C9 bond distance shortens to 2.126 Å. The CT from the isocyanide **1a** moiety to the **5a** fragment is 0.29 *e* during the C3−C9 bond construction. By crossing an energy barrier of 19.6 kcal mol^{-1}, intermediate **6a** is generated by exergonic of 13.3 kcal mol^{-1}. The resulting intermediate **6a** also exhibits the pronounced zwitterionic character, as demonstrated by the large charge accumulated on the isocyanide moiety (0.70 *e*) and dimethyl acetylenedicarboxylate fragment (−0.70 *e*). Both nucleophilicity (N = 4.71 eV) and electrophilicity (ω = 5.15 eV) of intermediate **6a** simulta-

dx.doi.org/10.1021/jo5017053 | J. Org. Chem. 2014, 79, 10811−10819

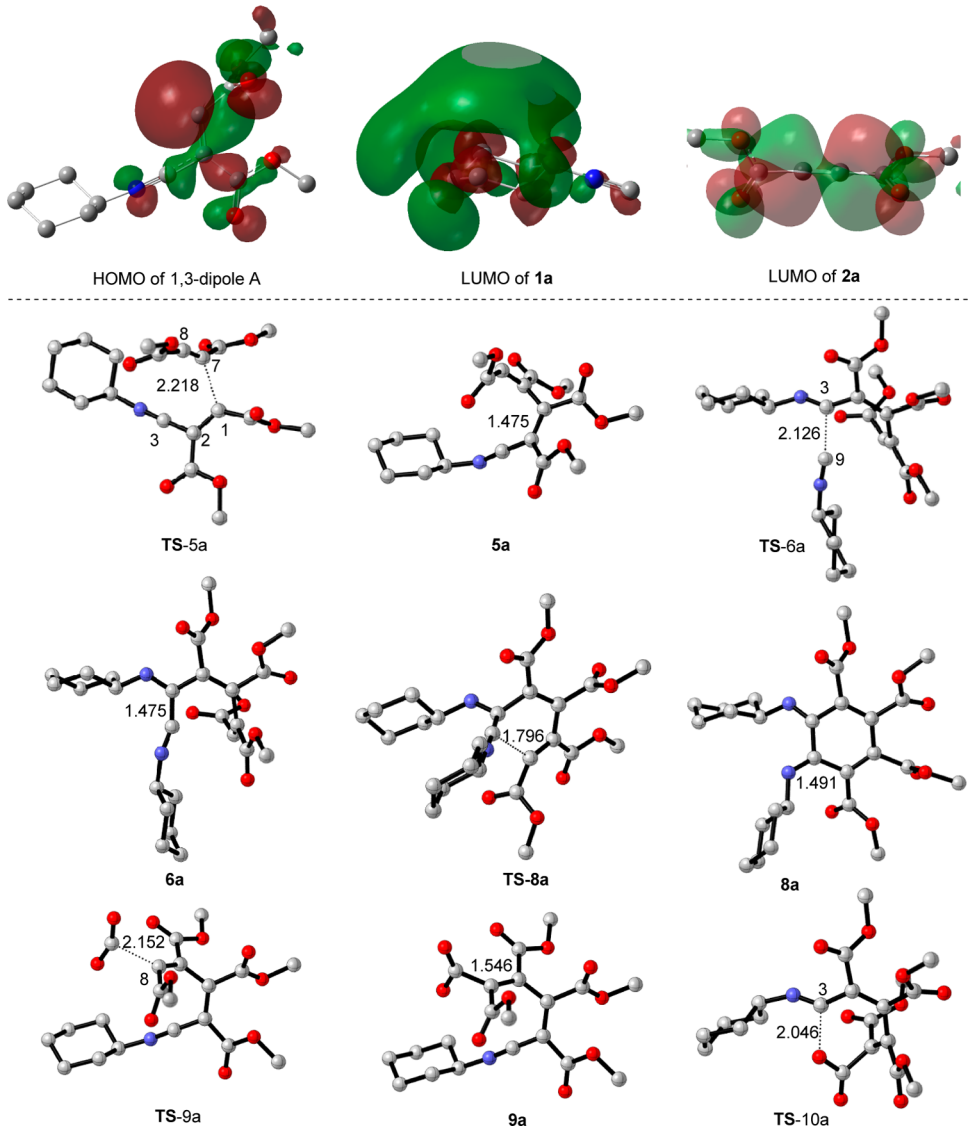

Figure 6. Visualization of molecular orbitals of the reactants, and the optimized structures of the species involved in formation of 1,5-dipole reaction channel.

neously increase as well. With this property, intermediate **6a** could undergo a rapid intramolecular cycloaddition transition state **TS**-8a, leaving the six-membered-ring cycloaddition product **8a** behind. Afterward, the cycloaddition product **8a** is yielded by exothermicity of 79.6 kcal mol^{-1}. Despite that the cycloaddition product **8a** was not detected in the experiment,[15] it is reasonable to predict that this species might be formed before intermediate **6a** was quenched by water. Additionally, similar to 1,5-dipole **5a**, zwitterionic intermediate **6a** with high nucleophilicity and electrophilicity may also carry out the intermolecular reaction with the external **1a**, **2a**, or CO_2, leading to the production of other side-products.

On the other hand, because abundant CO_2 is available in the reaction system, it could be captured by the strong nucleophile 1,5-dipole **5a** via transition state **TS**-9a, in which the bond distance between the C atom of CO_2 and the C8 atom shortens to 2.152 Å. The calculation predicts that the relative free energy of **TS**-9a is 11.6 kcal mol^{-1} lower than that of **TS**-6a, indicating that this carboxylation process is kinetically more advantageous than the electrophilic addition with the isocyanide **1a**. Consequently, it can be deduced that the generation of carboxylate **9a** is probably more preferred to the formation of zwitterionic intermediate **6a**, when 1,5-dipole **5a** is generated. Because of the zwitterionic character of carboxylate **9a**, the intramolecular nucleophilic addition from the electron-rich O atom of the carboxylate **9a** to the C3 atom via transition state **TS**-10a is considered. The seven-membered cycloaddition product **10a** could be afforded by crossing an energy barrier of 20.6 kcal mol^{-1} over transition state **TS**-10a. However, the seven-membered cycloaddition product **10a** with the large ring strain is 10.7 kcal mol^{-1} more unstable than **9a**, implying the reverse ring-opening process is thermodynamically favored.

In summary, it is apparent that the first step for the generation of 1,3-dipole **A** possesses the largest energy barrier of 24.3 kcal mol^{-1} and transition state **TS**-A is situated on the energy summit along the PES as well (Figure 2). Therefore, this step can be regarded as the rate-determining step (RDS) for the entire reaction, which is well compatible with the experimental observation that the reaction should be triggered at 80 °C.[15] Once 1,3-dipole **A** is formed, the subsequent evolution of this active species is vital for the distribution of the final products. The dual 1,3-dipolar cycloaddition reaction with CO_2 is faster

dx.doi.org/10.1021/jo5017053 | J. Org. Chem. 2014, 79, 10811−10819

than the competing electrophilic addition with dimethyl acetylenedicarboxylate **2a**. As a result, the spiro compound **4a** generated from the dual cycloaddition processes should be the major product, which is in good consistence with the experimental results.[15] From 1,5-dipolar intermediate **5a**, various side-products like zwitterionic species **6a**, cycloaddition product **7a**, and carboxylate **9a** would be yielded, which are accompanied by the dual 1,3-dipolar cycloaddition processes.

3.2. Substituent Effect on the Reaction. The understanding of the mechanism of the above reaction system motivates us to further investigate the utility and generality of this approach to synthesize dual cycloaddition spiro compound. As shown in Scheme 3, both isocyanides and alkynes with

Scheme 3. Isocyanides and Alkynes Used in the Present Theoretical Simulation

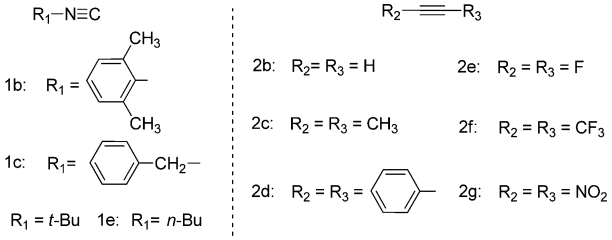

different substituents were employed as the substrates in the present theoretical simulation. On the basis of the computed results, it is clear that the entire reaction rate is determined by the energy barrier of formation of 1,3-dipolar species ($\Delta G_1^{\ddagger}$). The distribution of the final products should predominantly depend on the energy barrier gap ($\Delta\Delta G^{\ddagger}$) between the cycloaddition of 1,3-dipolar species with CO_2 ($\Delta G_{1,3}^{\ddagger}$) and the generation of 1,5-dipolar intermediate ($\Delta G_{1,5}^{\ddagger}$) step. Therefore, the intermediates and transition states involved in these critical steps were calculated in this section. The relative energy barriers of these steps are summarized in Table 1. To get a better understanding of the relationship between the structures and activities of the substrates, the electrophilicity and nucleophilicity indices of the isocyanides, alkynes, and 1,3-dipolar species are given in Table S6 of the Supporting Information.

Table 1. Relative Free Energies of the Transition States (in kcal mol^{-1}) in the Generation of 1,3-Dipolar Species, Lactone Intermediates, and 1,5-Dipolar Species in the Reaction of CO_2 with Various Isocyanides and Alkynes

reactants	$\Delta G_1^{\ddagger a}$	$\Delta G_{1,3}^{\ddagger}$	$\Delta G_{1,5}^{\ddagger}$	$\Delta\Delta G^{\ddagger}$
1a + **2a** + CO_2	24.3	13.5	16.8	3.3
1b + **2a** + CO_2	25.0	14.5	18.0	3.5
1c + **2a** + CO_2	25.0	14.1	16.8	2.7
1d + **2a** + CO_2	24.2	13.5	16.2	2.7
1e + **2a** + CO_2	24.1	13.8	16.7	2.9
1a + **2b** + CO_2	34.9		38.0	
1a + **2c** + CO_2	36.3		51.0	
1a + **2d** + CO_2	33.4	33.5	44.6	11.1
1a + **2e** + CO_2	15.5	−13.4	−10.6	2.8
1a + **2f** + CO_2	19.6	14.4	13.8	−0.6
1a + **2g** + CO_2	10.4	−13.7	−22.0	−8.3

[a] $\Delta G_1^{\ddagger}$, $\Delta G_{1,3}^{\ddagger}$, and $\Delta G_{1,5}^{\ddagger}$ are the free energies of the corresponding transition states relative to the zero-point. The sum of free energies of the reactants is set to zero-point.

To evaluate the substituent effect of isocyanides, the isocyanide **1a** was replaced by the experimentally used 2,6-dimerthylphenyl isocyanide **1b**, benzyl isocyanide **1c**, *tert*-butyl isocyanide **1d**, and *n*-butyl isocyanide **1e**, respectively. With respect to alkyl-substituted isocyanides (**1a**, **1d**, and **1e**), the nucleophilicities of **1b** and **1c** are slightly larger due to the conjugation effect from the adjacent aryl and benzyl groups. Nevertheless, the relative free energies of the transition states in the formation of 1,3-dipolar species ($\Delta G_1^{\ddagger}$) are not lowered, which implies that the substituents on the isocyanides play the weak impact on the 1,3-dipolar species generation. Moreover, the nucleophilicities of the resultant 1,3-dipolar species are also comparable to one another. As a result, the relative free energies of the transition states in the subsequent 1,3-dipolar cycloaddition steps ($\Delta G_{1,3}^{\ddagger}$), the generation of 1,5-dipolar intermediate steps ($\Delta G_{1,5}^{\ddagger}$), and the energy gaps ($\Delta\Delta G^{\ddagger}$) between these two steps are not obviously altered. The generation of the lactone intermediate should be kinetically more preferable to 1,5-dipolar intermediate, suggesting the desired dual 1,3-dioplar cycloaddition spiro compound would be obtained as the major product. The calculations reproduced the experimental results that isocyanides bearing cyclic aliphatic, aryl, alkyl substituents could be transformed to the corresponding dual 1,3-dioplar cycloaddition product under the present reaction conditions.[15]

In contrast, the substituents on the alkynes play the more significant roles on both reaction rate and selectivity to the final products. When the electron-withdrawing ester groups on the alkynes **2a** are substituted by the electron-donating hydrogen atoms and methyl groups, the electrophilicities of these two alkynes (**2b** and **2c**) are reduced. Thus, the relative free energies of the transition states in the formation of 1,3-dipolar species are remarkably increased from 24.3 to 34.9 and 36.3 kcal mol^{-1}, indicating that the higher reaction temperature is required when the electron-donating groups substituted alkyls are used as the substrates. Next, from the 1,3-dipolar species **1b-A**, all attempts to locate a **TS**-3a-like transition state for 1,3-dipolar cycloaddition of **1b-A** with CO_2 met failure, which might be due to the fact that the nucleophilicity of **1b-A** is so strong (N = 5.45 eV) that the PES is very flat. Furthermore, because the large negative charge on the C1 atom of the methyl-substituted 1,3-dipolar species **1c-A** could not be effectively dispersed, the *cis*-configurational structure, similar to the ester groups substituted 1,3-dipole **A**, always tends to the inactive three-membered-ring intermediate during the optimization. Instead, only the *trans*-configurational one could be located as a minimum. From the *trans*-configurational intermediate, the chemical fixation of CO_2 with the formation of the lactone intermediate proceeds through a stepwise mechanism (see Figure S4 in the Supporting Information). Relative to this process, the energy barrier for the formation of 1,5-dipolar species is high up to 51.0 kcal mol^{-1}, meaning the 1,5-dipolar species could not be generated under the present experimental condition.[15]

On the other hand, when another two alkynes **2d** and **2e** attached with the conjugate groups (−F and phenyl) are employed as the substrates, fluorine-substituted **2e** performs much better than phenyl-substituted **2d** in the generation of 1,3-dipolar species, as suggested by the much lower energy barrier (15.5 kcal mol^{-1}) for 1,3-dipole **1e-A**. The reason might be the electronegativity of fluorine atoms is larger than phenyl groups, making more positive charge accumulate on two C atoms of alkyne **2e** (0.27 *e* vs 0.00 *e* in **2d**). For the resultant

dx.doi.org/10.1021/jo5017053 | J. Org. Chem. 2014, 79, 10811−10819

1,3-dipolar species **1d-A** and **1e-A**, the nucleophilicity of **1d-A** is higher than that of **1e-A** due to the larger conjugation effect from phenyl groups. Hence, from phenyl-substituted 1,3-dipolar species **1d-A**, the cycloaddition with CO_2 takes an absolute advantage over the generation of 1,5-dipolar species ($\Delta\Delta G^{\ddagger}$ = 11.1 kcal mol^{-1}). For fluorine-substituted **1e**-A, the production of 1,5-dipolar species can not be avoided, as the energy gap between these two competing process is only 2.8 kcal mol^{-1}. Accordingly, it can be predicted that the aryl substituents favor the selectivity to 1,3-dipolar cycloaddition product, while fluorine substituents make the reaction proceed more easily.

Finally, when the ester groups of **2a** are substituted by the stronger electron-withdrawing groups ($-CF_3$ and $-NO_2$), the energy barrier for the formation of 1,3-dipolar species remarkably lowers as the electrophilicities of the alkynes **2f** and **2g** enhance. However, relative to 1,3-diploe species **A**, the nucleophilicities of the resultant 1,3-dipolar spices **2f-A** and **2g-A** dramatically decrease due to the stronger electron-withdrawing effect from $-CF_3$ and $-NO_2$ groups. From these two species, the relative free energies of the transition states in the step of 1,3-dipolar cycloaddition with CO_2 are larger than those in the nucleophilic addition with the alkynes, which means that the formation of the desired 1,3-dipolar cycloaddition product is kinetically unfavorable. Therefore, the alkynes with strong electron-withdrawing substituents should not be suitable for the synthesis of the spiro compounds.

4. CONCLUSIONS

The reaction mechanism of dual 1,3-dipolar cycloaddition of CO_2 with isocyanides and alkynes has been theoretically investigated by means of DFT calculations. The major conclusions are listed as follows:

The calculations show that the reaction starts from the nucleophilic attack of isocyanides to the electron-deficient alkynes with the formation of 1,3-dipolar species, which requires the largest energy barrier of 24.3 kcal mol^{-1} and is RDS for the entire reaction. Once this active species is generated, its subsequent 1,3-dipolar cycloaddition with CO_2, the homocoupling, and the intermolecular nucleophilic addition with dimethyl acetylenedicarboxylate will result in the different products. The 1,3-dipolar cycloaddition with CO_2 is 3.3 kcal mol^{-1} more preferable than the competing channel for the generation of 1,5-dipolar species in kinetics. As a result, the desired dual cycloaddition spiro compound is obtained with moderate yield, accompanied by the generation of several kinds of byproducts, such as zwitterionic species **6a**, hydrolysis product **7a**, cycloaddition product **8a**, and carboxylate **9a**.

The examinations of the substituent effect on both isocyanides and alkynes indicate that the generation of 1,3-dipolar species and selectivity to the final products are not sensitive to the substituents on isocyanides. On the contrary, the rate and selectivity of the reaction are very closely related to the substituents on the alkynes, which play the essential role in chemical reactivity and stabilization of 1,3-dipolar species. The alkynes attached with conjugate and moderate electron-withdrawing groups are predicted to be suitable for the production of the target spiro compounds under the present experimental conditions.

■ ASSOCIATED CONTENT

Supporting Information

Computational details, optimized geometries, calculated energies, and the full citation of the Gaussian 09 program. This material is available free of charge via the Internet at http://pubs.acs.org.

■ AUTHOR INFORMATION

Corresponding Author

*Tel.: +86-028-87727663. Fax: +86-028-87727663. E-mail: weiyili@mail.xhu.edu.cn.

Notes

The authors declare no competing financial interest.

■ ACKNOWLEDGMENTS

We are grateful for the financial support from the National Natural Science Foundation of China (no. 21402158), the Scientific Research Fund of Education Department of Sichuan Province (no. 14ZB0131), and the Key Scientific Research Found of Xihua University (no. Z1313319).

■ REFERENCES

(1) For reviews, see: (a) Sakakura, T.; Choi, J. C.; Yasuda, H. *Chem. Rev.* **2007**, *107*, 2365−2387. (b) Riduan, S. N.; Zhang, Y. *Dalton Trans.* **2010**, *39*, 3347−3357. (c) Aresta, M.; Dibenedetto, A. *Dalton Trans.* **2010**, *39*, 2975−2992. (d) Darensbourg, D. J. *Inorg. Chem.* **2010**, *49*, 10765−10780. (e) Omae, I. *Coord. Chem. Rev.* **2012**, *256*, 1384−1405. (f) Lu, X.; Darensbourg, D. J. *Chem. Soc. Rev.* **2012**, *41*, 1462−1484.

(2) (a) Ménard, G.; Stephan, D. W. *J. Am. Chem. Soc.* **2010**, *132*, 1796−1797. (b) Yu, D.; Zhang, Y. *Green Chem.* **2011**, *16*, 1275−1279. (c) Bontemps, S.; Vendier, L.; Sabo-Etienne, S. *Angew. Chem., Int. Ed.* **2012**, *51*, 1671−1674. (d) Dobrovetsky, R.; Stephan, D. W. *Angew. Chem., Int. Ed.* **2013**, *52*, 2516−2519. (e) Jacquet, O.; Frogneux, X.; Gomes, C. D. N.; Cantat, T. *Chem. Sci.* **2013**, *4*, 2127−2131. (f) Ueno, A.; Kayaki, Y.; Ikariya, T. *Green Chem.* **2013**, *15*, 425−430. (g) Wang, Y.; Sun, D.; Zhou, H.; Zhang, W.; Lu, X. *Green Chem.* **2014**, *16*, 2266−2277.

(3) (a) Lu, X.; Ren, W.; Wu, G. *Acc. Chem. Res.* **2012**, *45*, 1721−1735. (b) Song, Q.; He, L.; Wang, J.; Yasudab, H.; Sakakura, T. *Green Chem.* **2013**, *15*, 110−115. (c) Ren, Y.; Shim, J. J. *ChemCatChem* **2013**, *5*, 1344−1349. (d) Monassier, A.; D'Elia, V.; Cokoja, M.; Dong, H.; Pelletier, J. D. A.; Basset, J. M.; Kühn, F. E. *ChemCatChem* **2013**, *5*, 1321−1324. (e) Ema, T.; Miyazaki, Y.; Koyama, S.; Yano, Y.; Sakai, T. *Chem. Commun.* **2012**, *48*, 4489−4491. (f) Ma, J.; Song, J.; Liu, H.; Liu, J.; Zhang, Z.; Jiang, T.; Fan, H.; Han, B. *Green Chem.* **2012**, *14*, 1743−1748. (g) Castro-Gómez, F.; Salassa, G.; Kleij, A. W.; Bo, C. *Chem.—Eur. J.* **2013**, *19*, 6289−6298. (h) Anthofer, M. H.; Wilhelm, M. E.; Cokoja, M.; Markovits, I. I. E.; Pöthig, A.; Mink, J.; Herrmanna, W. A.; Kühn, F. E. *Catal. Sci. Technol.* **2014**, *4*, 1749−1758.

(4) (a) Zhou, H.; Zhang, W.; Liu, C.; Qu, J.; Lu, X. *J. Org. Chem.* **2008**, *73*, 8039−8044. (b) Van Ausdall, B. R.; Glass, J. L.; Wiggins, K. M.; Arif, A. M.; Louie, J. *J. Org. Chem.* **2009**, *74*, 7935−7942. (c) Kayaki, Y.; Yamamoto, M.; Ikariya, T. *Angew. Chem., Int. Ed.* **2009**, *48*, 4194−4197. (d) Riduan, S. N.; Zhang, Y.; Ying, J. Y. *Angew. Chem., Int. Ed.* **2009**, *48*, 3322−3325. (e) Gu, L.; Zhang, Y. *J. Am. Chem. Soc.* **2010**, *132*, 914−915. (f) Nair, V.; Varghese, V.; Paul, R. R.; Jose, A.; Sinu, C. R.; Menon, R. S. *Org. Lett.* **2010**, *12*, 2653−2655. (g) Huang, F.; Lu, G.; Zhao, L.; Li, H.; Wang, Z. *J. Am. Chem. Soc.* **2010**, *132*, 12388−12396. (h) Kelemen, Z.; Hollóczki, O.; Nagy, J.; Nyulászi, L. *Org. Biomol. Chem.* **2011**, *9*, 5362−5364. (i) Yang, L.; Wang, H. *ChemSusChem* **2014**, *7*, 962−998.

(5) Yang, Z.; He, L.; Gao, J.; Liu, A.; Yu, B. *Energy Environ. Sci.* **2012**, *5*, 6602−6639.

(6) (a) Gabriele, B.; Salerno, G.; Mancuso, R.; Costa, M. *J. Org. Chem.* **2004**, *69*, 4741−4750. (b) Wu, C.; Cheng, H.; Liu, R.; Wang, Q.; Hao, Y.; Yu, Y.; Zhao, F. *Green Chem.* **2010**, *12*, 1811−1816.

(7) (a) Feroci, M.; Orsini, M.; Sotgiu, G.; Rossi, L.; Inesi, A. *J. Org. Chem.* **2005**, *70*, 7795−7798. (b) Gu, Y.; Zhang, Q.; Duan, Z.; Zhang, J.; Zhang, S.; Deng, Y. *J. Org. Chem.* **2005**, *70*, 7376−7380. (c) Du, Y.; Wu, Y.; Liu, A.; He, L. *J. Org. Chem.* **2008**, *73*, 4709−4712. (d) Yang, Z.; Li, Y.; Wei, Y.; He, L. *Green Chem.* **2011**, *13*, 2351−2353.
(8) (a) Kimura, T.; Kamata, K.; Mizuno, N. *Angew. Chem., Int. Ed.* **2012**, *51*, 6700−6703. (b) Kimura, T.; Sunaba, H.; Kamata, K.; Mizuno, N. *Inorg. Chem.* **2012**, *51*, 13001−13008. (c) Ma, J.; Han, B.; Song, J.; Hu, J.; Lu, W.; Yang, D.; Zhang, Z.; Jiang, T.; Hou, M. *Green Chem.* **2013**, *15*, 1485−1489. (d) Zhao, Y.; Yu, B.; Yang, Z.; Zhang, H.; Hao, L.; Gao, X.; Liu, Z. *Angew. Chem., Int. Ed.* **2014**, *51*, 5922−5926.
(9) (a) Ion, A.; Doorslaer, C. V.; Parvulescu, V.; Jacobs, P.; Vos, D. D. *Green Chem.* **2008**, *10*, 111−116. (b) Kayaki, Y.; Suzuki, T.; Ikariya, T. *Chem.—Asian J.* **2008**, *3*, 1865−1870.
(10) (a) Menuel, S.; Porwanski, S.; Marsura, A. *New J. Chem.* **2006**, *30*, 603−608. (b) Wilson, A. A.; Garcia, A.; Houle, S.; Sadovski, O.; Vasdev, N. *Chem.—Eur. J.* **2011**, *17*, 259−264. (c) Hooker, J. M.; Reibel, A. T.; Hill, S. M.; Schueller, M. J.; Fowler, J. S. *Angew. Chem., Int. Ed.* **2009**, *48*, 3482−3485.
(11) Ansari, M. B.; Park, S. *Energy Environ. Sci.* **2012**, *5*, 9419−9437.
(12) (a) Gau, D.; Rodriguez, R.; Kato, T.; Saffon-Merceron, N.; de Cózar, A.; Cossío, F. P.; Baceiredo, A. *Angew. Chem., Int. Ed.* **2011**, *50*, 1092−1096. (b) Thammavongsy, Z.; Seda, T.; Zakharov, L. N.; Kaminsky, W.; Gilbertson, J. D. *Inorg. Chem.* **2012**, *51*, 9168−9170. (c) Dobrovetsky, R.; Stephan, D. W. *Angew. Chem., Int. Ed.* **2013**, *52*, 2516−2519. (d) Lescot, C.; Nielsen, D. U.; Makarov, I. S.; Lindhardt, A. T.; Daasbjerg, K.; Skrydstrup, T. *J. Am. Chem. Soc.* **2014**, *136*, 6142−6147.
(13) (a) Han, Z.; Rong, L.; Wu, J.; Zhang, L.; Wang, Z.; Ding, K. *Angew. Chem., Int. Ed.* **2012**, *51*, 13041−13045. (b) Courtemanche, M.-A.; Légaré, M.-A.; Maron, L.; Fontaine, F.-G. *J. Am. Chem. Soc.* **2013**, *135*, 9326−9329. (c) Huang, F.; Zhang, C.; Jiang, J.; Wang, Z.; Guan, H. *Inorg. Chem.* **2011**, *50*, 3816−3825.
(14) (a) Berkefeld, A.; Piers, W. E.; Parvez, M. *J. Am. Chem. Soc.* **2010**, *132*, 10660−10661. (b) Mitton, S. J.; Turculet, L. *Chem.—Eur. J.* **2012**, *18*, 15258−15262. (c) Wen, M.; Huang, F.; Lu, G.; Wang, Z. *Inorg. Chem.* **2013**, *52*, 12098−10107. (d) LeBlanc, F. A.; Piers, W. E.; Parvez, M. *Angew. Chem., Int. Ed.* **2014**, *51*, 789−792.
(15) Zhao, L.; Wang, S.; Xu, X.; Ji, S. *Chem. Commun.* **2013**, *49*, 2569−2571.
(16) (a) Becke, A. D. *J. Chem. Phys.* **1993**, *98*, 5648−5652. (b) Lee, C.; Yang, W.; Parr, R. G. *Phys. Rev. B* **1988**, *37*, 785−789. (c) Miehlich, B.; Savin, A.; Stoll, H.; Preuss, H. *Chem. Phys. Lett.* **1989**, *157*, 200−206.
(17) (a) Ditchfield, R.; Hehre, W. J.; Pople, J. A. *J. Chem. Phys.* **1971**, *54*, 724−728. (b) Hehre, W. J.; Ditchfield, R.; Pople, J. A. *J. Chem. Phys.* **1972**, *56*, 2257−2261. (c) Hariharan, P. C.; Pople, J. A. *Mol. Phys.* **1974**, *27*, 209−214. (d) Gordon, M. S. *Chem. Phys. Lett.* **1980**, *76*, 163−168. (e) Hariharan, P. C.; Pople, J. A. *Theor. Chem. Acc.* **1973**, *28*, 213−222. (f) Blaudeau, J. P.; McGrath, M. P.; Curtiss, L. A.; Radom, L. *J. Chem. Phys.* **1997**, *107*, 5016−5021. (g) Francl, M. M.; Pietro, W. J.; Hehre, W. J.; Binkley, J. S.; Gordon, M. S.; DeFrees, D. J.; Pople, J. A. *J. Chem. Phys.* **1982**, *77*, 3654−3655. (h) Buinning, R. C., Jr.; Curtiss, L. A. *J. Comput. Chem.* **1990**, *11*, 1206−1216. (i) Rassolov, V. A.; Pople, J. A.; Ratner, M. A.; Windus, T. L. *J. Chem. Phys.* **1998**, *109*, 1223−1229. (j) Rassolov, V. A.; Ratner, M. A.; Pople, J. A.; Redfern, P. C.; Curtiss, L. A. *J. Comput. Chem.* **2001**, *22*, 976−984.
(18) Marenich, A. V.; Cramer, C. J.; Truhlar, D. G. *J. Phys. Chem. B* **2009**, *113*, 6378−6396.
(19) (a) Grimme, S. *DFTD3, V3.0 Rev 1*; University Münster: Münster, Germany, 2013. (b) Grimme, S.; Antony, J.; Ehrlich, S.; Krieg, H. *J. Chem. Phys.* **2010**, *132*, 154104. (c) Grimme, S. *J. Comput. Chem.* **2006**, *27*, 1787−1799. (d) Grimme, S.; Ehrlich, S.; Goerigk, L. *J. Comput. Chem.* **2011**, *32*, 1456−1465. (e) Becke, A. D.; Johnson, E. R. *J. Chem. Phys.* **2005**, *123*, 154101. (f) Johnson, E. R.; Becke, A. D. *J. Chem. Phys.* **2005**, *123*, 24101. (g) Johnson, E. R.; Becke, A. D. *J. Chem. Phys.* **2006**, *124*, 174104.
(20) (a) Reed, A. E.; Weinhold, F. *J. Chem. Phys.* **1985**, *83*, 1736−1740. (b) Reed, A. E.; Weinstock, R. B.; Weinhold, F. *J. Chem. Phys.* **1985**, *83*, 735−746. (c) Reed, A. E.; Curtiss, L. A.; Weinhold, F. *Chem. Rev.* **1988**, *88*, 899−926. (d) Reed, A. E.; Schleyer, P. R. *J. Am. Chem. Soc.* **1990**, *112*, 1434−1445.
(21) (a) Domingo, L. R.; Sáez, J. A. *Org. Biomol. Chem.* **2009**, *7*, 3576−3583. (b) Domingo, L. R.; Chamorro, E.; Pérez, P. *J. Org. Chem.* **2008**, *73*, 4615−4624. (c) Parr, R. G.; von Szentpály, L.; Liu, S. *J. Am. Chem. Soc.* **1999**, *121*, 1922−1924. (d) Domingo, L. R.; José Aurell, M.; Pérez, P.; Contreras, R. *Tetrahedron* **2002**, *58*, 4417−4423. (e) Yamaguchi, Y.; Osamura, Y.; Schaefer, H. F. *J. Am. Chem. Soc.* **1983**, *105*, 7512−7516. (f) Parr, R. G.; Yang, W. *Density Functional Theory of Atoms and Molecules*; Oxford University Press: New York, 1989.
(22) The global electrophilicity index ω,[21c,d] which measures the stabilization energy when the system acquires an additional electronic charge ΔN from the environment, is given in terms of the electronic chemical potential μ and chemical hardness η by the following simple expression:[21e] $\omega = (\mu^2/2\eta)$. Both quantities can be calculated in terms of the HOMO and LUMO electron energies, ε_H and ε_L, as $\mu \approx (\varepsilon_H + \varepsilon_L)/2$ and $\eta \approx (\varepsilon_L - \varepsilon_H)$, respectively.[21f] The nucleophilicity index N,[21b] based on the HOMO energies obtained within the Kohn−Sham scheme, is defined as $N = E_{HOMO(Nu)} - E_{HOMO(TCE)}$.[21b] The nucleophilicity is taken relative to tetracyanoethylene (TCE) as a reference, because it has the lowest HOMO energy in a large series of molecules already investigated in the context of polar cycloadditions.
(23) Zhang, G.; Musgrave, C. B. *J. Phys. Chem. A* **2007**, *111*, 1554−1561.
(24) Frisch, M. J.; et al. *Gaussian 09*, revision A.02; Gaussian, Inc.: Wallingford, CT, 2009.
(25) Legault, C. Y. *CYLview, 1.0b*; Université de Sherbrooke: Sherbrooke, Québec, Canada, 2009; http://www.cylview.org.
(26) (a) Dömling, A. *Chem. Rev.* **2006**, *106*, 17−89. (b) Gulevich, A. V.; Zhdanko, A. G. R.; Orru, V. A.; Nenajdenko, V. G. *Chem. Rev.* **2010**, *110*, 5235−5331.